Origin and roles of oxygen impurities in hexagonal boron nitride epilayers

S. J. Grenadier, A. Maity, J. Li, J. Y. Lin, and H. X. Jiang[a)]
Department of Electrical and Computer Engineering, Texas Tech University, Lubbock, Texas 79409, USA

Photoluminescence emission spectroscopy and electrical transport measurements have been employed to study the origin and roles of oxygen impurities in hexagonal boron nitride (*h*-BN) epilayers grown on sapphire substrates. The temperature dependence of the electrical resistivity revealed the presence of a previously unnoticed impurity level of about 0.6 eV in *h*-BN epilayers grown at high temperatures. The results suggested that in addition to the common nitrogen vacancy (V_N) shallow donors in *h*-BN, oxygen impurities diffused from sapphire substrates during high temperature growth also act as substitutional donors (O_N). The presence of O_N gives rise to an additional emission peak in the photoluminescence spectrum, corresponding to a donor-acceptor pair recombination involving the O_N donor and the C_N (carbon occupying nitrogen site) deep level acceptor. Moreover, due to the presence of O_N donors, the majority charge carrier type changed to electrons in epilayers grown at high temperatures, in contrast to typical *h*-BN epilayers which naturally exhibit "p-type" character. The results provided a more coherent picture for common impurities/defects in *h*-BN as well as a better understanding of the growth mediated impurities in *h*-BN epilayers, which will be helpful for finding possible ways to further improve the quality and purity of this emerging material. *Published by AIP Publishing.*
https://doi.org/10.1063/1.5026291

Hexagonal boron nitride (h-BN) has attracted much interest due to its interesting fundamental properties and potential applications for deep-ultraviolet (DUV) optoelectronic materials,[1–16] solid state neutron detectors,[17–22] single photon emitters,[23,24] and graphene heterojunction devices.[25] Detectors fabricated from Boron-10 enriched *h*-BN epilayers have demonstrated the highest thermal neutron detection efficiency among solid-state neutron detectors to date of 58%.[26] However, it is still the least studied and understood among the members of the III-nitride material system. As with any emerging materials under development, the growth of *h*-BN epilayers with low defect densities is necessary to achieve technologically important practical devices. Previous studies have indicated that the formation energy of nitrogen vacancies (V_N) in *h*-BN is quite low and V_N and its related defects such as substitutional carbon impurities on the nitrogen site (C_N) are common impurities in *h*-BN.[27–33] Band-edge and impurity related photoluminescence (PL) emission spectroscopy studies revealed several impurity related emission peaks in *h*-BN epilayers, including a broad transition peak related to a donor-acceptor pair (DAP) transition near 4.1 eV together its replicas at about 3.9 and 3.7 eV and two other emission lines at around 5.3 eV and 5.5 eV (and their phonon replicas).[31–34] It was shown that it is possible to minimize or completely eliminate these impurity emission lines and to produce epilayers with pure free exciton emission at low temperatures by employing high NH_3 flow rates (or high V/III ratio) during *h*-BN epilayer growth,[34] supporting the hypothesis that these emission lines are related to the nitrogen vacancy (V_N) and its associated defects. Based on these experimental and previous theoretical studies, the broad peak covering from 3.7–4.1 eV and the

peak near 5.3 were assigned to DAP and *q*-DAP transitions[31–33] involving nitrogen vacancy shallow donors and two localized deep level acceptor states resulting from substitutional carbon impurities on nitrogen sites.[34]

More comprehensive studies on the impurity properties in *h*-BN for materials produced under different growth conditions are still needed to provide input for approaches towards the elimination of undesired defects and hence improvement of overall material quality. Analogous to AlN,[35] due to the strong bond between B and N, growing *h*-BN epilayers at relatively high temperatures is desired for obtaining *h*-BN with improved crystalline quality. Furthermore, building on previous knowledge for III-nitride epilayer growth, *h*-BN epilayers have been mostly grown on sapphire substrates. High growth temperatures together with the use of sapphire substrates unavoidably introduce oxygen impurities into *h*-BN films due to oxygen diffusion from sapphire substrates. However, detailed studies of the effects of oxygen impurities on the optical and electrical properties of *h*-BN epilayers are needed in order to provide insights into the roles of oxygen impurities in *h*-BN. In this work, we aim to probe such effects through PL emission and electrical transport measurements for *h*-BN epilayers deposited on sapphire substrates at different temperatures.

As shown schematically in the inset of Fig. 1, *h*-BN epilayers with a thickness of ~50 μm were grown by metal-organic chemical vapor deposition (MOCVD) on *c*-plane sapphire (Al_2O_3). The growth temperatures employed were between 1350 and 1500 °C, and hydrogen was used as a carrier gas. Due to the lattice mismatch between *h*-BN and Al_2O_3, a low temperature BN buffer layer of about 20 nm in thickness was deposited on the sapphire substrate prior to the growth of the *h*-BN epilayer. X-ray diffraction (XRD) measurements revealed that *h*-BN epilayers have a typical full width at half maximum (FWHM) of about 400 arc sec for the
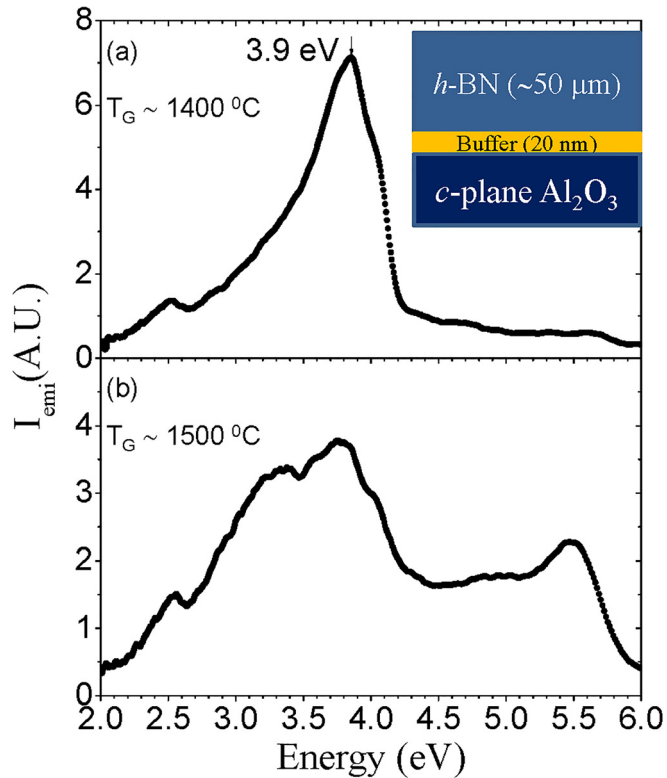
a)Email: hx.jiang@ttu.edu

FIG. 1. Room temperature PL spectra of *h*-BN epilayers deposited on sapphire by MOCVD at different growth temperatures (a) $T_G \sim 1400\,°C$ and (b) $T_G \sim 1500\,°C$. The inset shows a schematic of the *h*-BN epilayers used in this study.

h-BN (002) rocking curve, and secondary ion mass spectrometry (SIMS) results indicated that *h*-BN epilayers have a good stoichiometry.[7]

Figure 1 compares room temperature PL emission spectra of two *h*-BN epilayers, with one grown at a temperature of about 1400 °C and the other at about 1500 °C. The sample grown at 1400 °C consists of a dominant broad transition peak at about 3.9 eV. We believe that this 3.9 eV line has the same physical origin as the previously observed DAP transition peak superimposed within its phonon replicas covering from 3.7 to 4.1 eV, resulting from the recombination between the V_N (nitrogen vacancy) donor and the C_N (carbon on nitrogen site) deep acceptor. However, a new transition peak near 3.4 eV is clearly visible in the sample grown at a high temperature of 1500 °C. This transition peak also has a very board linewidth and a similar spectral lineshape as the transition peak near 3.9 eV, based on which we believe that this transition line has a similar physical nature as the 3.9 eV peak and hence attribute it to a DAP transition. From the energy difference between 3.9 eV and 3.4 eV and assuming the involved acceptor to be the same C_N, the involved donor in the 3.4 eV transition is expected to be about 0.5 eV deeper than the shallow donor of V_N.

To further understand the nature of the impurity giving rise to the 3.4 eV transition as well as its energy level, we attempted to measure the temperature dependence of the resistivity of the sample grown at 1500 °C. Due to the unique layered structure of *h*-BN and the difference in thermal expansion coefficients between *h*-BN and the sapphire substrate, *h*-BN

epilayers with a sufficient thickness tend to automatically separate from substrates during cooling down after growth, allowing the realization of freestanding and flexible *h*-BN wafers.[20,21] In order to characterize the electrical transport properties, *h*-BN epilayers were diced into pieces with lateral dimensions of $1\,mm \times 1\,mm$ and a Ni/Au $(10\,nm/20\,nm)$ bilayer was deposited on both sides of the $1\,mm \times 1\,mm$ freestanding samples using e-beam evaporation, as schematically shown in the inset of Fig. 2(a) to form photoconductive type of detectors. No post-deposition thermal annealing process was applied. Dark current and voltage characteristics at room temperature were probed, and a current density vs voltage (J-V) curve is plotted in Fig. 2(a) for a sample grown at 1500 °C. The results indicated that the Ni/Au bilayer provides an adequate Ohmic contact to *h*-BN despite the fact that undoped *h*-BN epilayers have a high resistivity ($\rho > 10^{14}\,\Omega\,cm$). Due to
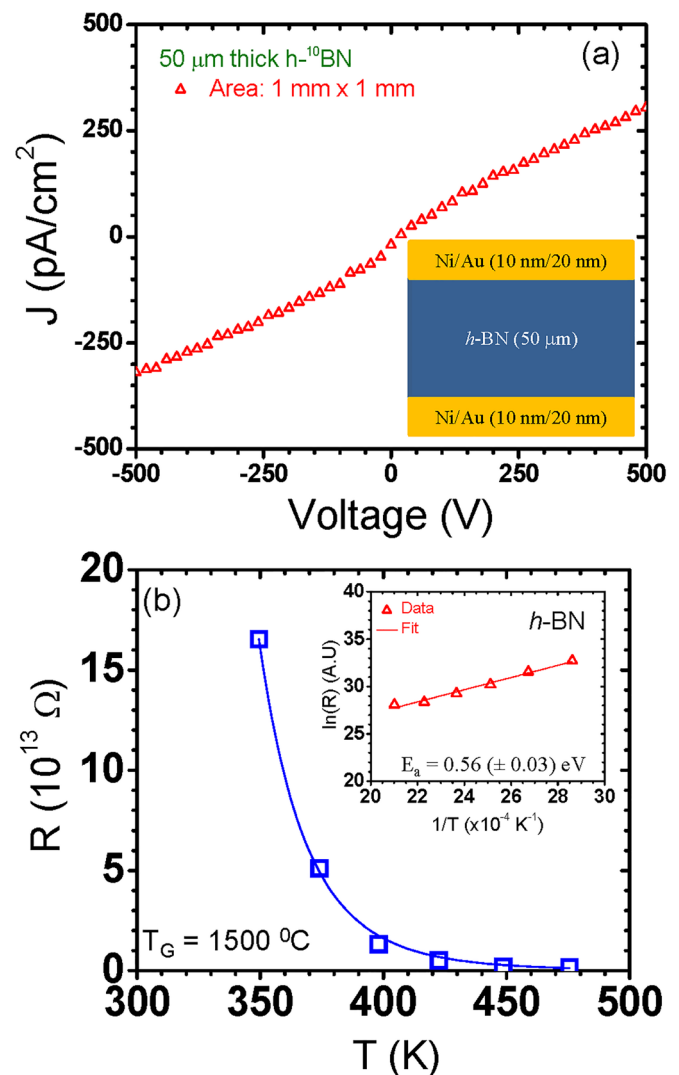

FIG. 2. (a) Room temperature current density vs voltage (J-V) characteristic of a freestanding *h*-BN sample grown at $\sim$1500 °C. The inset shows a schematic of the freestanding *h*-BN sample with a lateral dimension of $1\,mm^2$ and Ni/Au $(10\,nm/20\,nm)$ ohmic contacts deposited on both top and bottom surfaces used for electrical characterization. The thin Ni/Au $(10\,nm/20\,nm)$ bilayer is partially transparent to the incoming UV light. (b) The temperature dependence of the dark resistance of a freestanding *h*-BN sample grown at $\sim$1500 °C measured in the vertical direction (along the *c*-axis), and the inset shows the Arrhenius plot of the measured resistance providing a fitted activation energy of $0.56 \pm 0.03\,eV$.

this high resistive nature, probing directly the temperature dependence of the carrier concentration using Hall effect measurements was challenging. Figure 2(b) and the inset of Fig. 2(b) show the plots of the temperature dependence of the sample resistance (R) or equivalently resistivity (ρ) on the linear and semi-log (Arrhenius plot) scale, respectively, which follows the relation

$$R \sim \exp(E_a/k_B T), \quad \text{or} \quad \rho \sim \exp(E_a/k_B T), \qquad (1)$$

where E_a denotes the energy level of the involved impurity and K_B is Boltzmann's constant. In writing Eq. (1), we neglected any variations in the carrier mobility within the measurement temperature range. The Arrhenius plot of R provides a value of $E_a = 0.56\ (\pm 0.03)$ eV, as indicated in the inset of Fig. 2(b). Clearly, it is this impurity level that controls the dark current or resistivity of the *h*-BN epilayers grown at high temperatures. The previously measured energy levels of the two common defects of the V_N donor and the C_N acceptor in *h*-BN epilayers are about 0.1 eV and 2.3 eV, respectively.[31] Apart from these defects, oxygen diffusion from the sapphire substrate at high growth temperatures is likely to incorporate oxygen into *h*-BN during the growth. Being a group VI element, oxygen is expected to occupy the nitrogen site (O_N) acting as a donor. It is worth mentioning that the low temperature 20 nm thick buffer layer seems to be insufficient to block oxygen impurities from diffusing from the sapphire substrate, especially at high growth temperatures (above 1500 °C).

Based on the fact that the 3.4 eV emission line is absent in the epilayers grown at 1400 °C, we attribute the 3.4 eV DAP transition observed in Fig. 1 to the recombination between the O_N donor and the C_N acceptor. It is sensible to note that the energy level of O_N deduced from the PL spectra shown Fig. 1 is consistent with the electrical measurement results shown in Fig. 2. The two transition peaks near 3.9 and 3.4 eV observed in Fig. 1 are attributed to DAP transitions involving the same C_N acceptor. By neglecting any difference in the Coulomb energies caused by different donor concentrations, the energy difference between these two DAP transitions, 3.9 eV − 3.4 eV = 0.5 eV, can be attributed to the energy level difference between the two involved donors. With the understanding that the 3.9 eV DAP transition is due to the recombination between the V_N donor of about 0.1 eV below the conduction band and the C_N deep level acceptor, the observed spectral peak separation of 0.5 eV infers that the 3.4 eV DAP transition is related to O_N donors at about 0.6 eV below the conduction band. Given the fact that the observed 3.4 eV and 3.9 eV transitions are quite broad, the value of 0.6 eV estimated from the emission peak separation is in a reasonable agreement with the energy level of 0.56 eV deduced from the temperature dependence of the resistivity.

This interpretation is further corroborated by a very interesting observation that the majority charge carrier type in *h*-BN converts to electrons for materials grown at high temperatures. The mobility-lifetime ($\mu\tau$) product for holes is generally larger than that of electrons along the *c*-axis, implying that holes (electrons) behave like majority (minority) carriers in typical undoped *h*-BN.[20] Moreover, a previous

high-resolution angle-resolved photoemission spectroscopy study carried out on exfoliated *h*-BN also revealed that the valence-band maxima are located 2.5 eV below the Fermi level, further suggesting a residual *p*-type character of typical *h*-BN.[36] To characterize the $\mu\tau$ products, we make use of the unique property of the large optical absorption coefficient of about 7.5×10^5 cm^{-1} and hence a small optical absorption length of only about 14.5 nm in *h*-BN for the above bandgap excitation.[5,9] This implies that the incoming above bandgap photons will be completely absorbed within 70 nm ($\sim 5\lambda$) of the illuminated surface of *h*-BN and enables us to characterize $\mu\tau$ products for holes and electrons separately in thick *h*-BN epilayers, as illustrated in the insets of Fig. 3. Depending upon the polarity of the illuminated surface, specific charge carriers (hole or electron) can be selected for transport in the vertical direction (along the *c*-axis of *h*-BN). Negatively (positively) biased illuminated surface collects holes (electrons) immediately upon photo-excitation and allows only electrons (holes) to transport between the electrodes. Figures 3(a) and 3(b) compare the photocurrent-voltage characteristics of two *h*-BN samples grown at 1400 °C and 1500 °C. Fitting the photocurrents obtained in the configurations shown in the insets with modified Many's equation[37] below allows us to obtain the $\mu\tau$-products for holes and electrons for both samples[20,21]

$$I_i(V) = I_{0,i} \left[\frac{V \mu_i \tau_i \left(1 - e^{-\frac{L^2}{V \mu_i \tau_i}} \right)}{L^2 \left(1 + \frac{s_i L}{\mu_i V} \right)} \right]. \quad (i = e, h). \qquad (2)$$

Here, I_0 is the saturation current and $\mu_e\tau_e$ ($\mu_h\tau_h$) and s_e (s_h) denote the mobility-lifetime product and surface recombination velocity for electrons (holes), respectively.

As shown in Fig. 3, instead of holes being the usual majority carriers in typical *h*-BN epilayers grown at temperatures below 1400 °C in which $\mu_h\tau_h > \mu_e\tau_e$, electrons act as majority carriers in *h*-BN layers grown at 1500 °C in which $\mu_e\tau_e > \mu_h\tau_h$. We believe that this change in the majority carrier type from holes to electrons is due to the presence of increased concentration of oxygen donor impurities in *h*-BN samples grown on sapphire at high temperatures. It is reasonable to assume that the process of oxygen diffusion always takes place during growth at temperatures T < 1400 °C. However, for samples deposited at T < 1400 °C, the total concentration of acceptor-like defects is still higher than that of donors, whereas for samples grown on sapphire at high temperatures (T > 1500 °C), the total concentration of donors, such as V_N and O_N, is higher than that of acceptor-like defects. This is expected since the diffusion rate of oxygen impurities is expected to increase exponentially with the increase in the growth temperature.

The energy level of substitutional oxygen, O_N, has also been previously calculated and is about 0.33 eV below the conduction band.[38] Considering the energy gap difference between various calculation and measured values,[2,3,39,40] the measured value of ~ 0.56 eV here is in a reasonable range. Based on the PL and electrical transport results, we have constructed an energy diagram in Fig. 4 showing the estimated energy levels of common impurities/defects in *h*-BN epilayers, O_N, V_N, and C_N and their corresponding optical
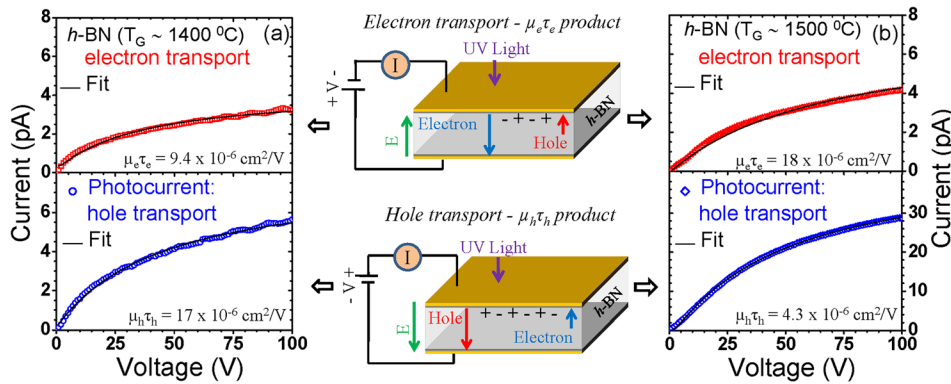
FIG. 3. Photocurrent-voltage characteristics of freestanding *h*-BN samples grown at (a) $\sim$1400 °C and (b) $\sim$1500 °C, and the solid curves are fittings using Eq. (2), which reveal that $\mu_h\tau_h > \mu_e\tau_e$ for the sample grown at $\sim$1400 °C and $\mu_e\tau_e > \mu_h\tau_h$ for the sample grown at $\sim$1500 °C. The inset shows the experimental geometries which enable the characterization of the electron and hole transport properties separately.

transitions. In constructing Fig. 4, we used a value of 6.4 eV for the energy bandgap of *h*-BN, as the band-to-band transition (and hence the bandgap) at $\sim$6.4 eV was directly observed in room temperature photocurrent spectra.[39,40] We believe that the results provided not only a more coherent picture for common impurities/defects in *h*-BN but also a better understanding of the growth mediated impurities and their effects on the optical and electrical properties of *h*-BN epilayers.

In summary, the origin and roles of oxygen impurities in *h*-BN epilayers have been studied via PL and electrical transport measurements. The results revealed that the combination of high temperature growth and the use of sapphire substrates introduced oxygen impurities in *h*-BN during MOCVD growth. These impurities occupy the nitrogen sites (O_N) and act as donors in *h*-BN. Consequently, the presence of O_N resulted in an additional optical transition near 3.4 eV in the PL emission spectra due to a DAP recombination involving the O_N donor and the C_N deep level acceptor and also changed the majority charge carrier type from holes to electrons. The PL and temperature dependence of the dark electrical resistivity revealed that the O_N donor in *h*-BN has an energy level of about 0.6 eV below the conduction band. It is important to note that common impurities/defects in *h*-BN identified so far are all related to the nitrogen vacancy (V_N), including V_N, O_N, and C_N. Therefore, finding effective ways to minimize the concentration of V_N will be important for further improvement of the material quality and purity of *h*-BN and the performance of *h*-BN devices.
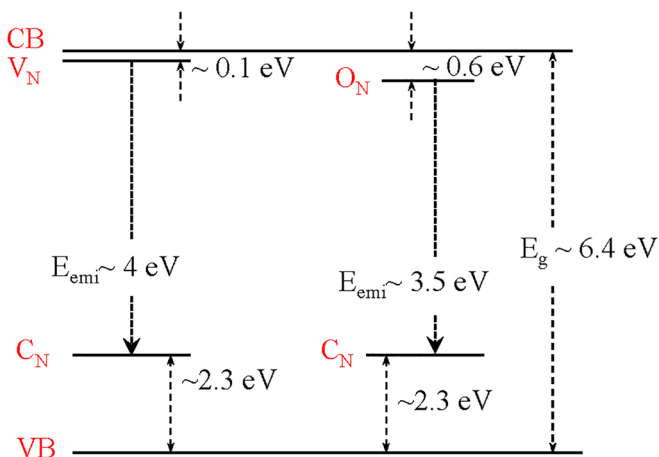

FIG. 4. Energy diagram indicating roughly the energy levels of common impurities/defects of V_N, O_N, and C_N and their corresponding optical transitions in *h*-BN epilayers.

[1]K. Watanabe, T. Taniguchi, and H. Kanda, Nat. Mater. **3**, 404 (2004).
[2]B. Arnaud, S. Lebègue, P. Rabiller, and M. Alouani, Phys. Rev. Lett. **96**, 026402 (2006).
[3]L. Wirtz, A. Marini, and A. Rubio, Phys. Rev. Lett. **96**, 126104 (2006).
[4]Y. Kubota, K. Watanabe, O. Tsuda, and T. Taniguchi, Science **317**, 932 (2007).
[5]T. Sugino, K. Tanioka, S. Kawasaki, and J. Shirafuji, Jpn. J. Appl. Phys., Part 2 **36**, L463 (1997).
[6]K. Watanabe and T. Taniguchi, Phys. Rev. B **79**, 193104 (2009).
[7]R. Dahal, J. Li, S. Majety, B. N. Pantha, X. K. Cao, J. Y. Lin, and H. X. Jiang, Appl. Phys. Lett. **98**, 211110 (2011).
[8]S. Majety, J. Li, X. K. Cao, R. Dahal, B. N. Pantha, J. Y. Lin, and H. X. Jiang, Appl. Phys. Lett. **100**, 061121 (2012).
[9]J. Li, S. Majety, R. Dahal, W. P. Zhao, J. Y. Lin, and H. X. Jiang, Appl. Phys. Lett. **101**, 171112 (2012).
[10]H. X. Jiang and J. Y. Lin, Semicond. Sci. Technol. **29**, 084003 (2014).
[11]D. A. Laleyan, S. Zhao, S. Y. Woo, H. N. Tran, H. B. Le, T. Szkopek, H. Guo, G. A. Botton, and Z. Mi, Nano Lett. **17**, 3738 (2017).
[12]X. Yang, S. Nitta, K. Nagamatsu, S. Y. Bae, H. J. Lee, Y. Liu, M. Pristovsek, Y. Honda, and H. Amano, J. Cryst. Growth **482**, 1 (2018).
[13]H. X. Jiang and J. Y. Lin, ECS J. Solid State Sci. Technol. **6**, Q3012 (2017).
[14]H. Liu, J. Meng, X. Zhang, Y. Chen, Z. Yin, D. Wang, Y. Wang, J. You, M. Gao, and P. Jin, Nanoscale **10**, 5559 (2018).
[15]X. Li, M. B. Jordan, T. Ayari, S. Sundaram, Y. E. Gmili, S. Alam, M. Alam, G. Patriarche, P. L. Voss, J. P. Salvestrini, and A. Ougazzade, Sci. Rep. **7**, 786 (2017).
[16]M. Sajjad, W. M. Jadwisienczak, and P. Feng, Nanoscale **6**, 4577 (2014).
[17]J. Uher, S. Pospisil, V. Linhart, and M. Schiebar, Appl. Phys. Lett. **90**, 124101 (2007).
[18]F. P. Doty, U.S. patent 6,727,504 (27 April 2004).
[19]T. C. Doan, S. Majety, S. Grenadier, J. Y. Lin, and H. X. Jiang, Nucl. Instrum. Methods Phys. Res. A **748**, 84 (2014).
[20]A. Maity, T. C. Doan, J. Li, J. Y. Lin, and H. X. Jiang, Appl. Phys. Lett. **109**, 072101 (2016).
[21]A. Maity, S. J. Grenadier, J. Li, J. Y. Lin, and H. X. Jiang, Appl. Phys. Lett. **111**, 033507 (2017).
[22]K. Ahmed, R. Dahal, A. Weltz, J. J.-Q. Lu, Y. Danon, and I. B. Bhat, Appl. Phys. Lett. **110**, 023503 (2017).
[23]R. Bourrellier, S. Meuret, A. Tararan, O. Stéphan, M. Kociak, L. H. G. Tizei, and A. Zobelli, Nano Lett. **16**, 4317 (2016).
[24]T. Q. P. Vuong, G. Cassabois, P. Valvin, A. Ouerghi, Y. Chassagneux, C. Voisin, and B. Gil, Phys. Rev. Lett. **117**, 097402 (2016).
[25]A. K. Geim and I. V. Grigorieva, Nature **499**, 419 (2013).
[26]A. Maity, S. J. Grenadier, J. Li, J. Y. Lin, and H. X. Jiang, J. Appl. Phys. **123**, 044501 (2018).
[27]B. Huang and H. Lee, Phys. Rev. B **86**, 245406 (2012).

[28]V. Wang, N. Ma, H. Mizuseki, and Y. Kawazoe, Solid State Commun. **152**, 816 (2012).

[29]C. Attaccalite, M. Bockstedte, A. Marini, A. Rubio, and L. Wirtz, Phys. Rev. B **83**, 144115 (2011).

[30]A. Zunger and A. Katzir, Phys. Rev. B **11**, 2378 (1975).

[31]M. G. Silly, P. Jaffrennou, J. Barjon, J. S. Lauret, F. Ducastelle, A. Loiseau, E. Obraztsova, B. Attal-Tretout, and E. Rosencher, Phys. Rev. B **75**, 085205 (2007).

[32]L. Museur and A. Kanaev, J. Appl. Phys. **103**, 103520 (2008).

[33]L. Museur, E. Feldbach, and A. Kanaev, Phys. Rev. B **78**, 155204 (2008).

[34]X. Z. Du, J. Li, J. Y. Lin, and H. X. Jiang, Appl. Phys. Lett. **106**, 021110 (2015); **108**, 052106 (2016).

[35]M. Imura, H. Sugimura, N. Okada, M. Iwaya, S. Kamiyama, H. Amano, I. Akasaki, and A. Bandoh, J. Cryst. Growth **310**, 2308 (2008).

[36]H. Henck, D. Pierucci, G. Fugallo, J. Avila, G. Cassabois, Y. J. Dappe, M. G. Silly, C. Chen, B. Gil, M. Gatti, F. Sottile, F. Sirotti, M. C. Asensio, and A. Ouerghi, Phys. Rev. B **95**, 085410 (2017).

[37]A. Many, J. Phys. Chem. Solids **26**, 575 (1965).

[38]F. Oba, A. Togo, I. Tanaka, K. Watanabe, and T. Taniguchi, Phys. Rev. B **81**, 075125 (2010).

[39]T. C. Doan, J. Li, J. Y. Lin, and H. X. Jiang, Appl. Phys. Lett. **109**, 122101 (2016).

[40]M. R. Uddin, J. Li, J. Y. Lin, and H. X. Jiang, Appl. Phys. Lett. **110**, 182107 (2017).